Voltage-Gated Ion Channels

2

Lori Isom, Gustavo Patino, Luis Lopez-Santiago, and Yukun Yuan

Abbreviations

BACE1	β-site amyloid precursor protein-cleaving enzyme 1
Ca^{2+}	Calcium
CAM	Cell adhesion molecule
CaMKII	Calcium/calmodulin-dependent protein kinase II
cDNA	Complementary deoxyribonucleic acid
Cl^-	Chloride
CNS	Central nervous system
ENa	Sodium equilibrium potential
ERK	Extracellular-signal regulated kinases
Ff	Fraction of channels that inactivate through fast inactivation
FHF	Fibroblast growth factor homologous factors
Fr	Fraction of channels that have recovered from inactivation
Fs	Fraction of channels that inactivate through slow inactivation
g	Conductance

L. Isom (✉)
Pharmacology, Molecular and Integrative Physiology, University of Michigan, Ann Arbor, MI, USA
e-mail: lisom@umich.edu

G. Patino
Neuroscience Program, Pharmacology, University of Michigan, Ann Arbor, MI, USA
e-mail: gapatino@umich.edu

L. Lopez-Santiago
Pharmacology, University of Michigan, Ann Arbor, MI, USA
e-mail: lopezslf@umich.edu

Y. Yuan
Pharmacology, University of Michigan, Ann Arbor, MI, USA
e-mail: yukuny@umich.edu

D.W. Pfaff (ed.), *Neuroscience in the 21st Century*,
DOI 10.1007/978-1-4614-1997-6_3,

$GEFS^+$	Genetic (generalized) epilepsy with febrile seizures plus
GPD1L	Glycerol-3-phosphate dehydrogenase 1-like protein
I	Current
ICD	Intracellular domain
Ig	Immunoglobulin
IP5P	Inositol polyphosphate 5-phosphatase
Ipeak	Peak current
iPSCs	Induced pluripotent stem cells
K^+	Potassium
MAPK	Mitogen-activated protein kinases
MOG1	Multicopy suppressor of gsp1
mRNA	Messenger ribonucleic acid
Na^+	Sodium
NF	Neurofascin
Nr-CAM	Neuronal cell adhesion molecule
PCR	Polymerase chain reaction
PDZ	Post synaptic density protein, Drosophila disk large tumor suppressor, Zonula occludens-1 protein
PNS	Peripheral nervous system
PP2A	Protein phosphatase 2A
PTPH1	Protein tyrosine phosphatase H1
REST	RE1-silencing factor
RPTPβ	Receptor phosphoprotein tyrosine phosphatase-β
Src	Sarcoma
t	Time
TM	Transmembrane
τf	Rate constant for fast inactivation
τr	Rate constant for recovery
τs	Rate constant for slow inactivation
TTX	Tetrodotoxin
V	Voltage
VGCC	Voltage-gated calcium channels
VGPC	Voltage-gated potassium channels
VGSC	Voltage-gated sodium channels
Vm	Membrane voltage membrane potential

Brief History

Electrical signaling by ion channels is a fundamental cellular regulatory pathway in all organisms from prokaryotes to humans. Voltage-gated Na^+ (VGSC), Ca^{2+} (VGCC), and K^+ (VGPC) channels are responsible for action potential generation in electrically excitable cells, for example, neurons and muscle cells, and for

regulation of membrane potential and intracellular Ca^{2+} levels in other cell types. The basic functional properties of this protein family were initially defined in classic voltage-clamp studies by Hodgkin and Huxley in 1952. During the 1970s, many scientists built upon the fundamental insights of these pioneers to investigate electrical signal transduction using patch-clamp techniques, to measure ion channel function by neurotoxin-activated ion flux, and to detect VGSC proteins (the first member of this family to be studied biochemically) by high affinity binding of the neurotoxins tetrodotoxin, saxitoxin, and scorpion toxin (discussed later in this chapter). However, the molecular basis of excitability remained unclear until the 1980s, when Dr. William A. Catterall and his colleagues at the University of Washington discovered the VGSC protein (in 1980) and the VGCC protein (in 1984).

Dr. Catterall's key paper published in 1980 first revealed the protein subunits of VGSCs expressed in mammalian brain: a principal α subunit and auxiliary β subunits. Subsequent experiments resulted in purification of brain VGSCs, demonstrating that they comprise a heteromeric complex of three subunits: α of 260 kDa, β1 of 36 kDa, and β2 of 33 kDa. These important VGSC experiments were the first to identify a voltage-gated ion channel protein and the first to characterize an ion channel complex of principal and auxiliary subunits, a structural theme that was subsequently found to be repeated for the VGCCs and VGPCs (Fig. 2.1). Several laboratories then used this protein chemistry information to identify VGSC genes, resulting in cloning of the first VGSC α subunit cDNA from the electric eel electroplax by Professor Shosaku Numa and colleagues at Kyoto University in 1984 and subsequent homology cloning of mammalian brain VGSCs in 1986 by Dr. Norm Davidson's group at the California Institute of Technology. Dr. Catterall's group subsequently defined the primary structures and physiological functions of VGSC β1 and β2 subunits, using a combination of protein purification and cDNA cloning, in 1992 and 1995, respectively. In this chapter, we will use VGSCs as prototypic channels from which the fields of voltage-gated ion channel biochemistry and molecular biology arose. Many of the concepts introduced here for VGSCs are applicable to the family of voltage-gated ion channels.

Since the initial discovery of VGSC proteins, the voltage-gated ion channel family has expanded to number over 143 in the human genome. Members of this diverse family are responsible for electrical excitability; control of synaptic transmission, secretion, and contraction; sensory signal transduction; regulation of cell membrane potential; cell-cell adhesion; transepithelial transport of ions and other solutes; and osmotic homeostasis in plants and prokaryotes. Structure-function studies, including the crystal structure of a bacterial VGSC, have given clear insight into the molecular mechanisms of channel voltage-dependent activation and inactivation gating processes and their modulation by drugs, neurotransmitters, hormones, and neurotoxins. Heterologous expression of channel cDNAs in transfected cell lines, followed by the generation of knockout and knock-in mouse models, has led to a greater understanding of the roles of these important proteins in physiology and pathophysiology. Identification of human mutations in voltage-gated ion

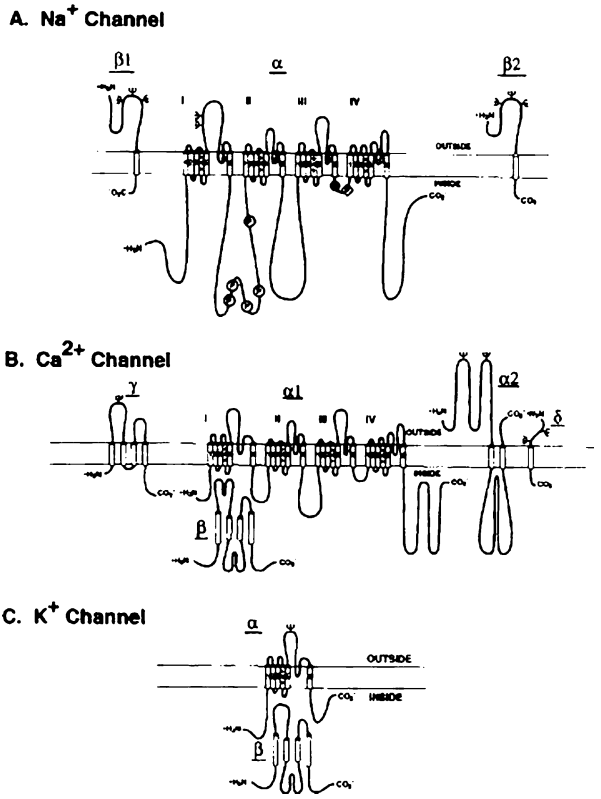

Fig. 2.1 Transmembrane organization of voltage-gated ion channel subunits. Membrane topologies, the subunits of voltage-gated ion channels, are illustrated. Cylinders represent predicted alpha-helical segments. *Bold lines* represent the polypeptide chains of each subunit, with length approximately proportional to the number of amino acid residues. Ψ, sites of predicted N-linked glycosylation; P, sites of demonstrated protein phosphorylation (Reproduced with permission from Neuron, Vol. 12, 1183–1194, June, 1994)

channel genes opened the field of ion channelopathies. Recently, new technologies, for example, the induced pluripotent stem cell technique, have provided even greater opportunities for scientists and physicians to understand the role of voltage-gated ion channels in human excitable cells and to develop novel therapeutic agents targeting these proteins to treat devastating ion channel-associated diseases like epilepsy and cardiac arrhythmia. Thus, discovery of the first members of the voltage-gated ion channel protein family and establishment of fundamental principles of their structure, function, regulation, and molecular pharmacology represent major advances in neuroscience.

Introduction

The ability of some types of mammalian cells to fire an action potential – to change their membrane potential in response to stimuli – is vital to their physiological function. We call these cells "excitable." Although traditionally this ability has only

been ascribed to cells like neurons and muscle cells, we now know that other cell types can also be excitable under certain conditions, including pancreatic β cells, leucocytes, and even metastatic cancer cells. Changes in membrane potential result from the flow of ions down their concentration gradient from one side of the plasma membrane to the other. The ions most commonly involved in this process are Na^+, K^+, Ca^{2+}, and Cl^-. Because ions are charged and water soluble, and plasma membranes are composed of hydrophobic lipids, ions must cross through specialized protein structures that traverse the membrane and form water-filled pores. These specialized proteins are called ion channels. In some cases, for example, VGSCs, a single protein forms the ion-conducting pore. In other cases, VGPCs or nicotinic receptor channels, a number of protein subunits must assemble to form the pore structure. Depending on the stimulus required for pore opening, or activation, channels can be classified as voltage dependent (channels that open in response to changes in membrane voltage), ligand gated (channels that open in response to the binding of a neurotransmitter, hormone, or drug), signal transduction dependent (channels that open in response to the binding of an intracellular second messenger), or mechanosensitive (channels that open in response to changes in the shape and/or tension of the cell membrane). This chapter describes voltage-gated ion channels. As explained above, we will focus our description on one group of channels in the voltage-gated ion channel family: the VGSCs.

As we learned in previous chapters, the interior of neurons is negatively charged, and the membrane potential is negative under resting conditions. Concentrations of Na^+ and Ca^{2+} outside the cell are higher than inside the cell. Concentrations of K^+ inside the cell are higher than outside the cell. When the membrane potential becomes less negative, or is depolarized, VGSCs and VGCCs open, allowing the flow of ions down their concentration gradients into the cell. Similarly and simultaneously, the opening of VGPCs allows K^+ to flow out of the cell. Some specialized VGCCs and VGPCs function slightly differently and will not be discussed in detail here. For example, some VGPCs are opened when the interior of the cell is made more negative than the resting potential, or is hyperpolarized. In this case, K^+ flows into the cell to restore the membrane potential back to its resting value. Some specialized VGCCs open at membrane potentials that are equal to or below the resting membrane potential. The flow of Ca^{2+} into the cell in response to the opening of these channels results in increasing the membrane potential to a value where other VGSCs and VGPCs can be activated. In this way, these specialized VGCCs serve as pacemakers. While we will focus on VGSCs in this chapter, many of the structural and physiological principles that we will discuss are also true for VGCCs and VGPCs.

VGSCs Are Multimeric Protein Complexes Containing α and β Subunits

Ion channels contain a water-filled pore that traverses the cell membrane. For VGSCs a single α subunit forms this ion-conducting pore. Molecular cloning efforts have revealed that there are nine different genes that encode VGSC α subunits in

Table 2.1 Nomenclature of VGSC subunits

Gene name	Protein name	Tissue expression	TTX sensitivity
α subunits			
SCN1A	$Na_v1.1$	CNS and PNS neurons, heart	+
SCN2A	$Na_v1.2$	CNS and PNS neurons	+
SCN3A	$Na_v1.3$	CNS and PNS neurons (high expression during fetal brain development), heart	+
SCN4A	$Na_v1.4$	Skeletal muscle	+
SCN5A	$Na_v1.5$	Heart, CNS neurons	–
SCN8A	$Na_v1.6$	CNS and PNS neurons, astrocytes, Schwann cells, heart	+
SCN9A	$Na_v1.7$	PNS sensory neurons, Schwann cells, neuroendocrine cells	+
SCN10A	$Na_v1.8$	PNS sensory neurons	–
SCN11A	$Na_v1.9$	PNS sensory neurons	–
β subunits			
SCN1B	β1/β1B	CNS and PNS neurons, heart, skeletal and smooth muscle, astrocytes, Schwann cells, Bergmann glia, kidney, liver	N/A
SCN2B	β2	CNS and PNS neurons, heart, skeletal and smooth muscle, astrocytes	N/A
SCN3B	β3	CNS and PNS neurons, heart, skeletal muscle, kidney, liver	N/A
SCN4B	β4	CNS and PNS neurons, heart, skeletal and smooth muscle, Bergmann glia, kidney, liver	N/A

CNS central nervous system, *PNS* peripheral nervous system, *N/A* Not applicable

mammals, including humans. These subunits are expressed in brain, peripheral nerve, heart, skeletal muscle, and other excitable cells (Table 2.1). A certain neuron or cardiac myocyte, for example, can express a number of different VGSC α subunits, resulting in a particular pattern of excitability. VGSC α subunits associate with accessory β subunits, proteins that do not form the pore, but regulate how the pore opens and closes, where the pore-forming α subunit is expressed at the plasma membrane, how much channel protein is expressed, and in some cases which drugs modify channel behavior. Mammalian β subunits are encoded by four different genes, whose products are widely expressed in multiple tissues (Table 2.1), including, very interestingly, some that are not known to express α subunits. This suggests that β subunits also have roles that are independent of ion conduction. One limitation of the literature exploring the tissue expression of VGSC subunits is that many of these studies relied on the use of polymerase chain reaction, or PCR. We know now that there is a poor correlation between mRNA levels and protein levels of VGSC subunits, so changes in mRNA may not reflect changes in protein. In brain, we have learned using protein assays, starting with Dr. Catterall's early work, that α subunits are associated with one covalently linked β subunit (β2 or β4)

Table 2.2 Proteins interacting with VGSCs

Extracellular matrix	Cytoskeleton	Membrane	Cytosolic	Cell adhesion molecules
Tenascin C	Ankyrin G	$K_v4.2$	MOG1	Contactin
Tenascin-R	Ankyrin B	$K_v4.3$	14-3-3η	NF-155
	Telethonin	RPTPβ	FHF	NF-186
	Plakophilin-2	Caveolin-3	Calmodulin	N-cadherin
	α1-syntrophin	VDAC3V	CaMKII	Nr-CAM
	β-actin	Synaptotagmin	Fyn kinase	
	Dystrophin		GPD1L	
	βIV spectrin		p11	
			Moesin	
			Tetraspanin	
			Dynein	
			IP5P	
			TAO2	
			Nedd4-like ubiquitin-protein ligases	

CaMKII $Ca^{2\pm}$/calmodulin-dependent protein kinase II, *FHF* fibroblast growth factor homologous factors, *GPD1L* glycerol-3-phosphate dehydrogenase 1-like protein, *IP5P* inositol polyphosphate 5-phosphatase, *MOG1* multicopy suppressor of *gsp1*, *NF* neurofascin, *RPTPβ* receptor tyrosine phosphatase β

and one non-covalently linked β subunit (β1 or β3). In this way, VGSCs are called heterotrimers. The exact partners of each α subunit, including specific β subunits, likely depend on cell type and subcellular location within that cell. The proper functioning of α-β subunit complexes requires interaction with other transmembrane, cytoskeletal, extracellular matrix, and signal transduction proteins (Table 2.2). The nature of these protein-protein interactions is also specific to cell type and, within a given cell, to a particular subcellular compartment. For example, a given VGSC α subunit may have different electrical properties when expressed at the neuronal axon initial segment vs. when expressed in the cardiac t-tubule. The importance of VGSC protein-protein interactions is highlighted by the observation that mutations in the genes encoding non-channel proteins involved in these complexes can result in VGSC dysfunction and human disease (see below) and that the symptoms of these diseases are similar to those caused by direct mutation of VGSC genes.

To add to this complexity, VGSCs are regulated at the transcriptional level and mRNA splice variants of α and β subunit genes are developmentally regulated. The exact transcription factors and regulatory networks that are important in these processes are still under investigation. We do know that the RE1-silencing transcription factor (REST) is a developmental regulator of VGSC α subunit genes (where it promotes) and the gene encoding β3 (where it inhibits) expression. In addition, we know that expression of β3 protein is induced by p53.

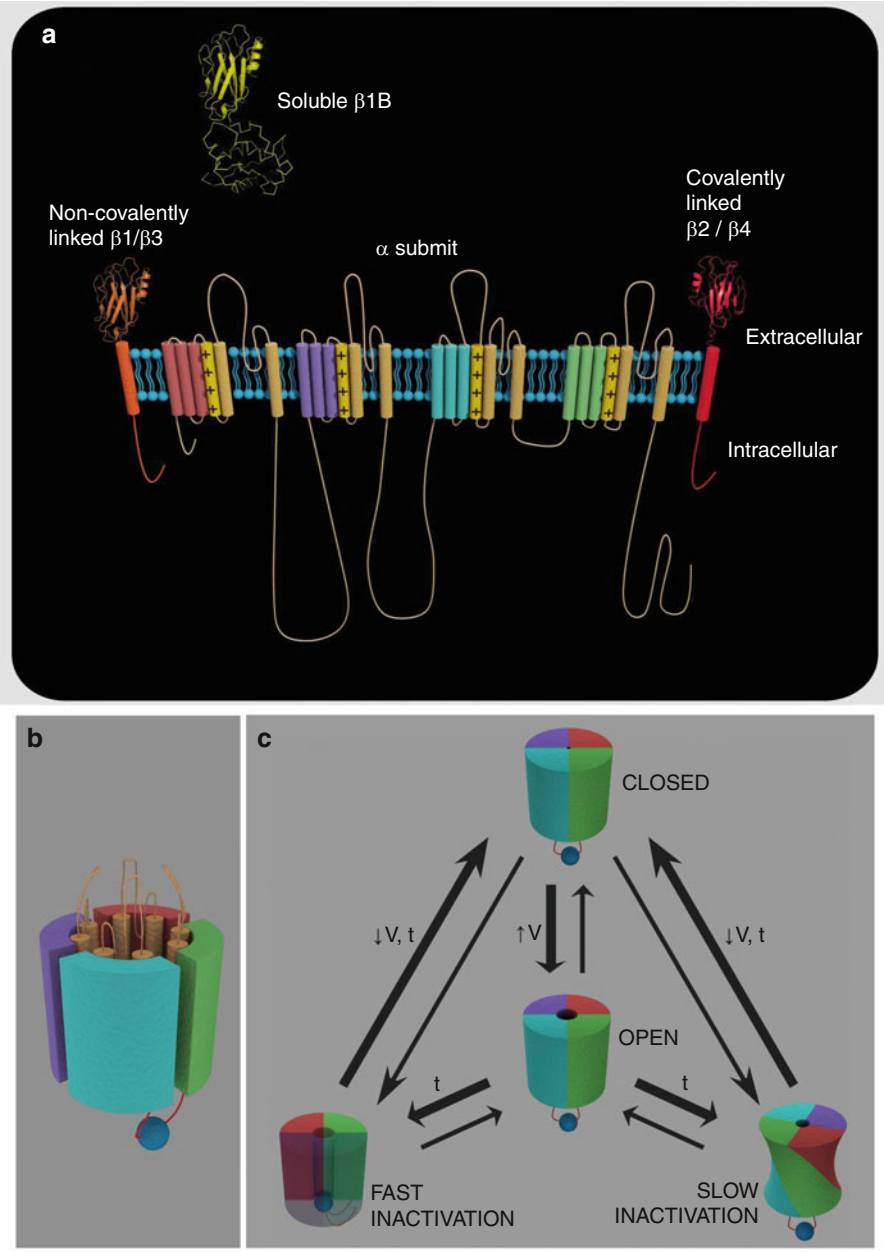

Fig. 2.2 (**a**) *VGSC topology*. VGSC α subunits are composed of 24 transmembrane (TM) segments grouped into four domains of six TM segments each. The first three TM segments of each domain are colored *pink* (domain I), *purple* (DII), *cyan* (DIII), and *green* (DIV), respectively. The fourth TM segment in each domain is the voltage sensor (*yellow*), while the fifth and sixth TM segments line the pore of the channel (orange). The intracellular linker domain between DIII and

Changes in the Conformation of VGSC α Subunits Determine the State of the Channel

VGSC α subunits are polytopic glycoproteins composed of 1792–2009 amino acids that migrate on SDS polyacrylamide gels at a relative molecular weight of approximately 260 kDa. Each VGSC α subunit contains 24 transmembrane segments grouped into four homologous domains (DI to DIV), of six transmembrane segments each (S1–S6) (Fig. 2.2a). The transmembrane segments in each domain come together to form a columnar structure, while the four domains fold together in pseudo-tetrafold symmetry to form the ion-conducting pore (Fig. 2.2b). VGCCs have a similar, single α subunit structure. In contrast, VGPCs are composed of four separate α subunit proteins, each containing six transmembrane segments, which must associate to form the ion-conducting pore. This allows for greater diversity in VGPC structure. In all voltage-gated channels, the extracellular loop between transmembrane segments S5 and S6 in each domain "dips" into the plasma membrane, inserting into the lipid bilayer (Fig. 2.2a). These domains compose the face of the channel structure that lines the pore. In VGSCs, amino acids donated from each of the four homologous domains form a ring that confers ion selectivity of the pore to Na+. A similar mechanism holds true for Ca^{2+} in VGCCs and for K^+ in VGPCs. This does not mean that other cations cannot flow through the VGSC pore. However, this does mean that, for example, in VGSCs, Na^+ fits into the selectivity filter at lowest energy and thus flows at a much higher rate than any other cation. When the channel is closed, or in the resting state, the pore domains do not allow the flow of any ion.

In all voltage-gated ion channels, transmembrane segment S4 in each domain is composed of a series of positively charged residues at intervals of three amino acids within the α-helix. Under resting conditions, positively charged S4 amino acids are buried within the cell membrane. Upon depolarization of the cell interior, the S4 helical segments are postulated to rotate up and out through the membrane toward the extracellular face. For VGSCs, this "sliding helix" model of voltage-dependent gating postulates that the S4 α-helical segments serve as transmembrane voltage sensors that are driven outward by membrane depolarization. In this model, the

Fig. 2.2 (continued) DIV is the inactivation gate. VGSC β subunits are transmembrane (β1, β2, β3, or β4) or secreted (β1B) proteins. The transmembrane β subunit proteins are either covalently linked (β2 or β4) or non-covalently linked (β1 or β3) to the α subunit. (**b**) The four domains of the α subunit come together to form the channel, with the fifth and sixth TM segments of each domain forming the walls of the ion-conducting pore. The extracellular domains between the fifth and sixth TM segments of each domain form the ion selectivity filter. Each of the domains is indicated in the same color as in **a**. (**c**) VGSCs can transition between the closed, open, fast-inactivated, or slow-inactivated states. Membrane depolarization (↑V) favors the transition between closed and open states (*wide arrows*). The channel transitions to one of the inactivated states in spite of ongoing membrane depolarization. The transition from the inactivated to the close state is favored by time and membrane repolarization (↓V). However, transitions in the opposite directions can still occur (*thin arrows*) (Figures courtesy of Mauricio Patino)

gating charges are stabilized within the plasma membrane by formation of ion pairs with nearby negatively charged residues. Exchange of these ion pair partners catalyzes the transmembrane movement of the gating charges in response to membrane potential changes. This sliding movement of the S4 segments is thought to cause opening of the pore and flow of Na^+ ions down their concentration gradient. (Note that other models, including a paddle model of the voltage sensors of K^+ channels, have been proposed; however, the recently published crystal structure of a bacterial VGSC by the Catterall laboratory supports the sliding helix model.) This is termed channel activation, resulting in the channel open state. This state mediates the action potential upstroke in most excitable cells.

Voltage-gated ion channels inactivate (or cease conducting ions) immediately after they are activated. Again, we will use VGSCs as an example. VGSC inactivation occurs within 1 ms of channel opening, even though the membrane remains depolarized. The VGSC inactivation gate has been identified as the short intracellular loop connecting DIII and DIV of the α subunit. A hydrophobic motif of three amino acids (isoleucine-phenylalanine-methionine) serves as an intracellular pore blocker that folds into the mouth of the pore in a "hinged lid" model. The inactivation gate is then stabilized in the pore by interaction with the channel carboxyl-terminal domain. Genetic diseases of hyperexcitability are often caused by impaired VGSC inactivation (as discussed below). Because this structural change takes place rapidly, it is called fast inactivation. In addition to this process, a change in the disposition of the four homologous domains occurs that reduces the size of the pore to stop ion flow. Because this structural change requires longer periods of time to occur, we call this slow inactivation. In general, VGSCs do not transition from inactivated states to open states. Instead, channels must first convert into the closed state before reopening. This transition occurs after a period of time required for the cell membrane to repolarize, called the refractory period. After channels reach the closed state, they are again ready to open or activate (Fig. 2.2c).

VGSC States and Na^+ Current Properties

The hallmark of all voltage-gated ion channels is their regulation on the millisecond timescale by changes in membrane voltage through two gating processes: activation and inactivation. This electromechanical transduction process is responsible for electrical signal transduction and propagation throughout biology and is thus essential for life. Here we will again use VGSCs as a representative example.

The flow of Na^+ ions through VGSCs results in an electrical Na^+ current that can be measured in the laboratory. Na^+ currents expressed by a variety of mammalian cells (including dissociated cells and organotypic slices) and from cell lines that have been transfected with α subunits can be recorded using the patch-clamp technique. To study Na^+ current characteristics using this method, the membrane potential of the cell or membrane patch is "held" at different values (this is called

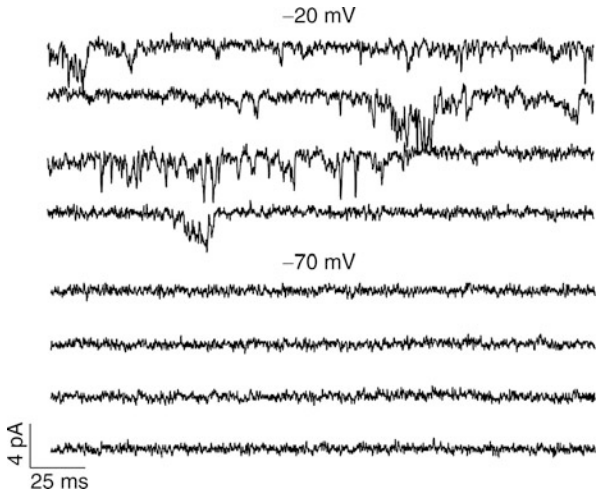

Fig. 2.3 *Na^+ currents in an inside-out patch from a cortical pyramidal neuron in response to different voltages*. Single-channel signals were recorded using an Axopatch 200B amplifier and an IBM-type computer run pClamp 10.0 software (Axon Instruments). The electrode tip was coated with Sylgard 184 (Dow Chemicals) and fire polished to 5–8 MΩ when filled with internal solution containing (in mM): 150 N-methyl-D-glucamine, 4 NaCl, 0.5 $CaCl_2$, 10 EGTA-CsOH, 10 HEPES, 2 Mg-ATP, and 0.4 GTP (pH 7.2 titrated with CsOH). The external solution contained (in mM): 125 NaCl, 2.5 KCl, 1 $MgCl_2$, 1.25 KH_2PO_4, 26 $NaHCO_3$, 2 $CaCl_2$, 10 TEA-Cl, 0.2 $CdCl_2$, and 25 mM D-glucose (pH 7.35–7.4 saturated with 95% O2/5% CO2 at room temperature). The membrane potential was held at −90 mV. Signals were low-pass filtered at 1 KHz. By convention, a downward deflection indicates inward current

voltage clamp), and the resulting current is recorded. As described above, membrane depolarization changes the channel state from closed to open. This explanation is actually an oversimplification. In reality, VGSCs transition rapidly between states in a bidirectional manner (from closed to open and vice versa, open to inactivated and vice versa, inactivated to closed and vice versa), and such changes are stochastic in nature (Fig. 2.2c). This can be observed in the laboratory using single-channel recording techniques in which membrane patches, held even at the resting potential, show occasional Na^+ currents. When the membrane is depolarized, the probability of the channel transitioning from closed to open increases; thus, under these conditions, the majority of channels transition to the open state, resulting in more frequent Na^+ currents (Fig. 2.3, *upper panel, −20 mV*). Following depolarization, some channels remain closed, while other transition back from open to the closed state. Overall, however, most channels open. In a whole-cell voltage-clamp recording, in which we observe the sum of many Na^+ currents through individual channels, we obtain a curve similar to those shown in Figs. 2.4a and 2.6a. By convention, a downward deflection indicates inward current. Notice that the current amplitude (indicated in milliamps on the Y axis) increases with time (indicated as milliseconds on the X axis) as more and more channels transition from closed to open and predominate over channels going

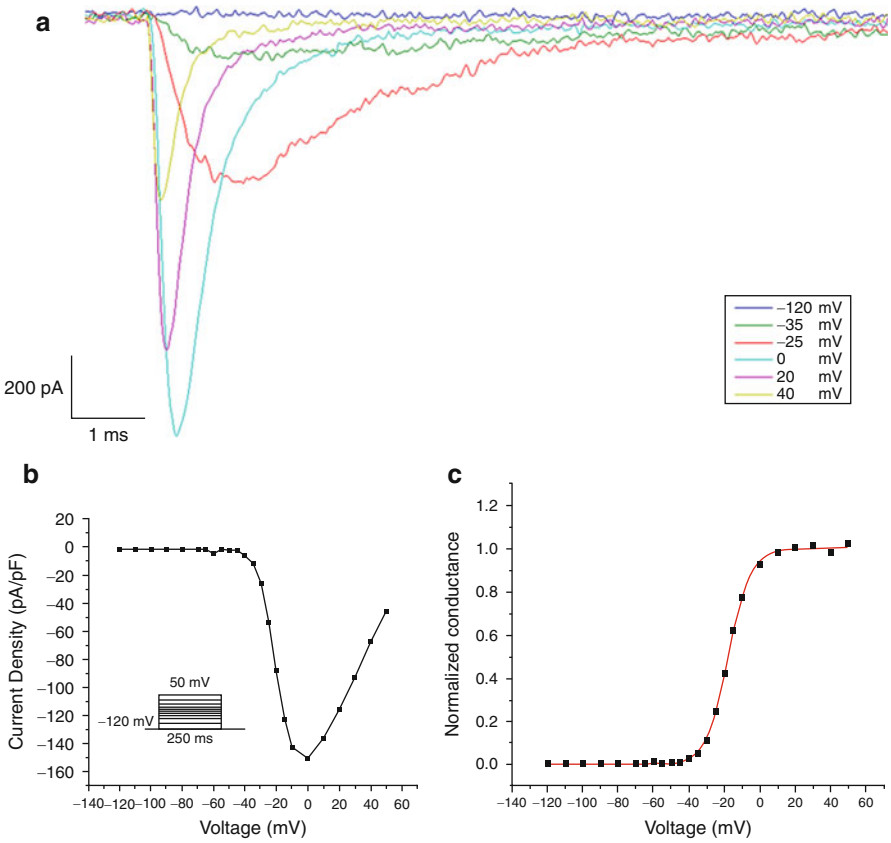

Fig. 2.4 *Na^+ current density and voltage dependence of activation.* (**a**) Na^+ currents recorded using the whole-cell patch-clamp technique in response to holding a cell expressing VGSCs at different membrane voltages. (**b**) Current density plot of peak Na^+ currents obtained at different membrane voltages (inset). (**c**) Voltage dependence of activation plot of peak Na^+ conductance obtained using the same protocol as the inset in **b**

from open to closed or from open to inactivated. The current reaches a maximum, called the peak current amplitude. At this point, the maximum number of channels are in the open state for that given voltage, and the probability of channels transitioning from closed to open is highest. In milliseconds, that number begins to decrease as most open channels transition into the inactivated state.

When a depolarized potential is reached at which 100% of the available channels are recruited to transition from closed to open, experimentally raising the membrane potential to an even higher value will not result in further increases in current. Na^+ flows into the cell both because its concentration is normally higher outside than inside (a chemical driving force) and because the inside of the cell is normally more negative than the outside (an electrical driving force). As more Na^+ enters the cell, the electrical driving force gradually dissipates and reaches zero. At this point, the electrical driving force reverses and begins to counteract the chemical

driving force. Finally, these two forces balance each other, resulting in no net Na^+ flow. At this point, the amplitude of the Na^+ current is zero. The voltage at which this balance is achieved is called the Na^+ equilibrium potential (ENa) and has been experimentally determined to be 60–90 mV in most mammalian neurons, depending on the intracellular concentration of Na+. We refer to the electrochemical driving force for Na^+ as that which is equal to the membrane voltage (Vm) minus ENa. Notice that at more depolarized potentials, the driving force becomes reduced. When we hold the membrane voltage at increasingly depolarized potentials, we observe that the peak Na^+ current also increases until the membrane potential reaches a point between −20 and 0 mV. Thus, greater membrane depolarization results in more channels that are activated. This compensates for a driving force that is becoming progressively smaller. The voltage at which we obtain the highest level of peak current corresponds to that where the greatest number of channels transitioning from closed to open compensate for the decreasing electrochemical driving force. At higher potentials, the Na^+ current amplitude begins to decrease, until it reaches a point where membrane voltage equals ENa and the driving force is zero (Fig. 2.4a). Because cells of different sizes have varying amounts of membrane surface area and thus contain varying numbers of VGSCs, peak Na^+ current is usually normalized to the cell membrane capacitance, which is used as a proxy for cell size. This normalized value is called current density and is often presented in a current–voltage (I-V) curve (Fig. 2.4b).

We can analyze the percentage of channels activated at a given voltage by plotting the voltage dependence of current activation. To generate this plot, we first convert each peak current to conductance (g) by dividing the value of the peak current by the driving force:

$$g = \mathrm{Ipeak}/(\mathrm{Vm} - \mathrm{ENa}).$$

The values of g for the different voltages are then normalized to the highest value obtained, which corresponds to the voltage with the highest peak current. By plotting normalized conductance values vs. voltage, we know the voltage dependence of activation (Fig. 2.4c).

The portion of Na^+ current following the point of peak current can be analyzed to determine the kinetics of fast and slow inactivation. This is performed experimentally by fitting that segment of the curve to the equation:

$$I = (Fs \times e - t/\tau s) + (Ff \times e - t/\tau f) + C,$$

where I is the value of the Na^+ current, Fs and Ff are the fractions of channels that inactivate through slow and fast inactivation, respectively, t is time from the peak current, and τs and τf are rate constants for slow and fast inactivation, respectively. τ refers to the time at which 63% of the channels are inactivated and 37% are still open. Therefore, τs is the time at which 63% of the channels that will show slow inactivation have stopped passing current. The higher the value of τ, the slower the channels will inactivate and the wider the trace of the Na^+ current. Some channels

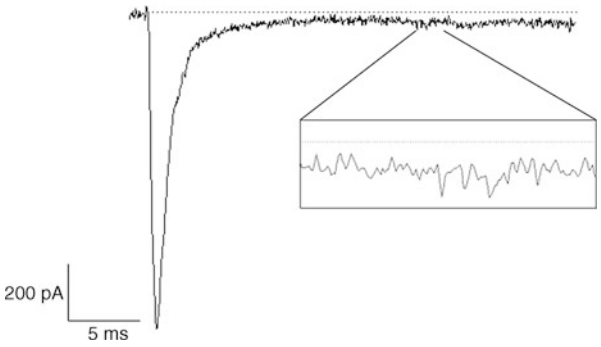

Fig. 2.5 *Persistent Na^+ current*. Persistent Na^+ current recorded using the whole-cell patch-clamp technique. Inset shows the zoom-in of the marked area

do not exhibit inactivation and continue allowing the flow of ions as long as the stimulus, or the experimental voltage pulse, is present. Current that persists after all channels that were going to inactivate have done so is called the persistent current (Fig. 2.5) and is indicated in the above formula by the value C. Another way to analyze the persistent current is to average the Na^+ current value at the end of the recording period over a given amount of time and express that value as a percentage of the peak current. As stated above, defective channel inactivation and changes in the level of persistent current are associated with ion channelopathies.

One can experimentally determine the proportion of channels that are inactivated at each voltage. To accomplish this, the membrane potential is first held under voltage clamp at a given voltage (called the prepulse) for a specific period of time (usually three to five times the slowest τ of inactivation measured, such that the prepulse is sufficient to achieve steady state), during which channels inactivate. Immediately after the prepulse, the holding potential of the membrane is changed to a depolarized voltage, at which 100% of the channels are expected to be activated (this is called the test pulse, Fig. 2.6a, inset). Remember, to increase the probability of channels opening following inactivation, channels must first transition into the closed state. This only happens with high probability after the membrane has been repolarized for a certain amount of time. Since in this experiment, the membrane is not repolarized between the prepulse and the test pulse, channels that have been inactivated have a very low probability of transitioning back to the open state and do not pass current. Further, only the population of channels that have not been activated by the prepulse will open with the test pulse. Therefore, at very low voltage prepulses, that activate very few channels, the test pulse will elicit high peak currents. In contrast, high voltage prepulses will result in peak currents close to zero during the test pulse (Fig. 2.6a). If the peak current values measured during the test pulse are normalized to the highest values obtained and then these normalized values are plotted against prepulse voltages, the voltage dependence of inactivation relationship is generated (Fig. 2.6b). Note that both the voltage dependence of activation and voltage dependence of inactivation plots have sigmoidal shapes. In the area of intersection of these curves is a triangular region corresponding to a range of voltages at which a proportion of channels are being

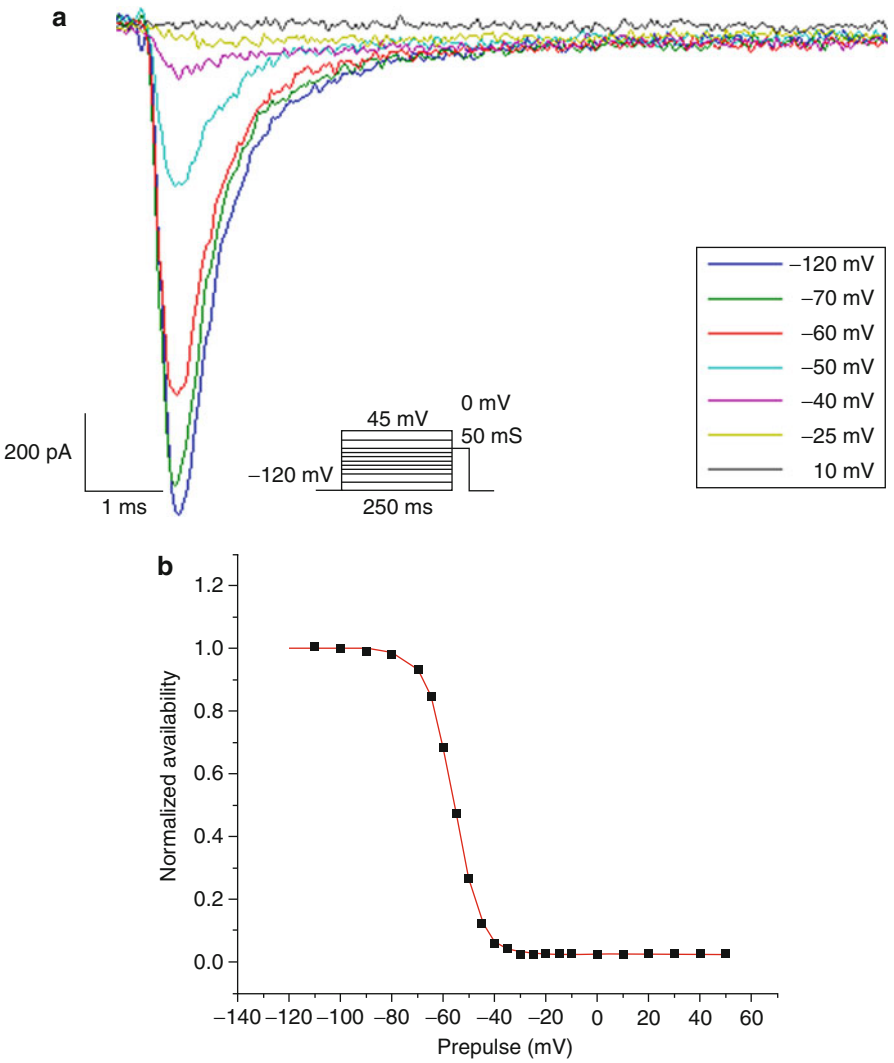

Fig. 2.6 *Voltage dependence of inactivation.* (**a**) Na^+ currents recorded using the whole-cell patch-clamp technique. A cell expressing VGSCs was held at the indicated membrane voltages (prepulse) and then stimulated by changing the voltage to elicit the highest peak current (test voltage). The inset shows the protocol used. (**b**) Voltage dependence of inactivation plot of peak Na^+ currents obtained during the test voltage using the same protocol as the inset in **a**

activated, but not all channels are being inactivated. When the membrane potential is held at voltages within this range, channels can transition back and forth between open and inactivated states, resulting in a current called the window current.

Another parameter that can be determined experimentally is the rate with which inactivated channels transition to the closed state, from which they are

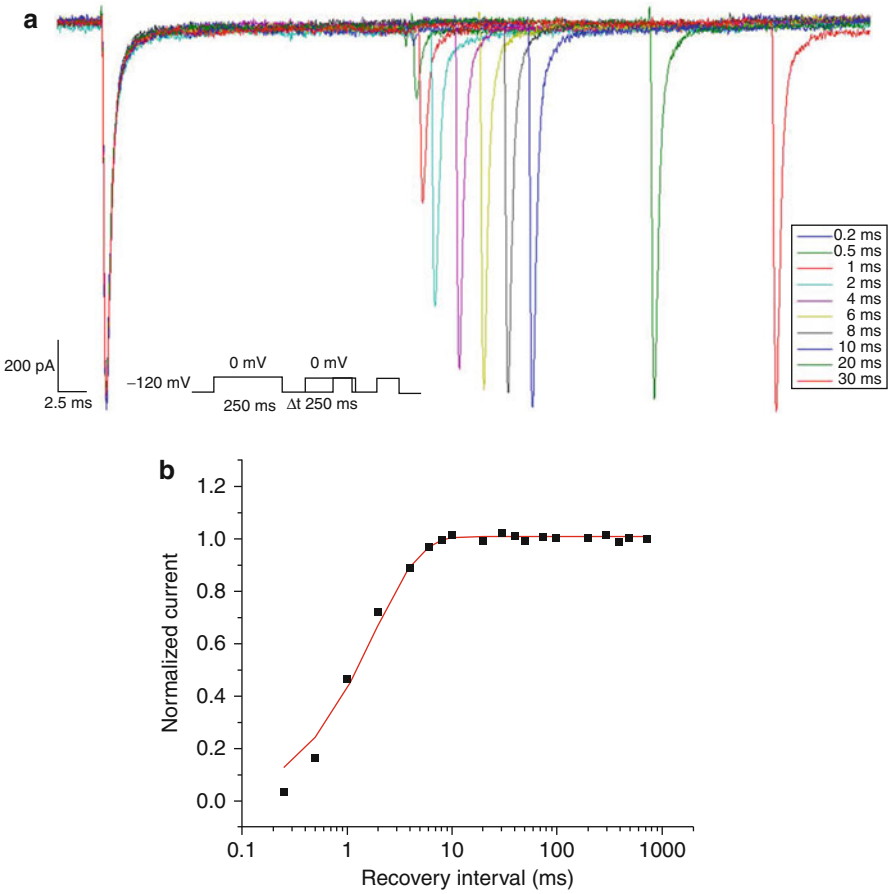

Fig. 2.7 *Recovery from inactivation.* (**a**) Na^+ currents recorded using the whole-cell patch-clamp technique, holding a cell expressing VGSCs at a given membrane voltage (prepulse), returning the cell back to the resting membrane potential for different time intervals, and then stimulating the cell to the same voltage as the prepulse (test pulse). The inset shows the protocol used. (**b**) Time dependence of recovery plot of peak Na^+ currents obtained during the test pulse normalized to the peak current obtained during the prepulse

again available to be activated by a depolarizing pulse. To accomplish this, a voltage-clamp experiment is performed in which a prepulse is given to a voltage that will activate, and then inactivate, a majority of the channels. The Na^+ current elicited by the prepulse is recorded. The membrane is then hyperpolarized for variable periods of time, after which a test pulse is given to the same voltage as the prepulse, and the elicited Na^+ current is recorded. If the time between the two pulses is too brief for inactivated channels to transition to the closed state, these channels cannot be activated during the test pulse. As this time period increases, more and more channels are able to transition to the closed state and thus become activated by the test pulse (Fig. 2.7a). By plotting the peak current

at the test pulse normalized to the peak current at the prepulse vs. the time interval, we obtain the kinetics of recovery from inactivation (Fig. 2.7b). We can calculate the tau of recovery, i.e., the time at which 63% of the channels have recovered from inactivation, by fitting this curve to the formula:

$$\mathrm{Fr} = 1 - \mathrm{e}(-\mathrm{t})/\tau\mathrm{r},$$

where Fr is the fraction of channels that have recovered from inactivation, t is the time interval, and τr is the tau for recovery.

Voltage-gated Na^+ currents underlie the rising phase of the action potential in excitable cells, including neurons and myocytes. Experimentally, we can determine how changes in Na^+ current influence the action potential by again using the patch-clamp technique. For this experiment, whole-cell recordings are made from excitable cells by passing current of known amplitude and measuring how the membrane voltage changes in response. This technique is called current clamp. Using this methodology, we can measure important action potential parameters, including threshold, slope, amplitude, and duration. Importantly, we can also measure the firing rate and firing patterns of excitable cells. A more detailed discussion of action potentials is found in subsequent chapters.

Effects of β Subunits on Na^+ Current

Using heterologous expression systems, many investigators have shown that VGSC β subunits can modify the voltage dependence and kinetic characteristics of α subunits by, for example, changing the peak current amplitude, voltage dependence of activation and/or inactivation (and thus the window current), rate of inactivation, recovery from inactivation, and/or the level of persistent current. The accessory subunits of VGCCs and VGPCs (Fig. 2.1) function in a similar manner in terms of modifying the electrophysiological characteristics of the channel pore. For VGSC β subunits, β1–β4, when coexpressed with VGSC α subunits in mammalian cells in vitro, are capable of modulating some or all of these current characteristics in a manner that is dependent on the particular α subunit expressed. The carboxyl-terminus of β4 is unique among the VGSC β subunits because a peptide representing this region can produce a specialized type of Na^+ current termed resurgent current in native cells. In this voltage-clamp experiment, after channels have opened in response to depolarization, but before inactivating, the pore can be blocked by the carboxyl-terminal β4 peptide, stopping the flow of ions. Upon repolarization, the β4 peptide is expelled from the pore, allowing ion flow to resume and generating a brief Na^+ current prior to channel closure or inactivation (Fig. 2.8). Thus, the β4 carboxyl-terminal region has been postulated to be a VGSC pore-blocking particle causing resurgent current in vivo, although this has yet to be demonstrated conclusively. Resurgent Na^+ current is known to play a critical role in the excitability of cerebellar Purkinje neurons and nociceptive neurons in dorsal root ganglia. Taken together, these data suggest a complex regulation of Na^+ current by β subunits acting in concert.

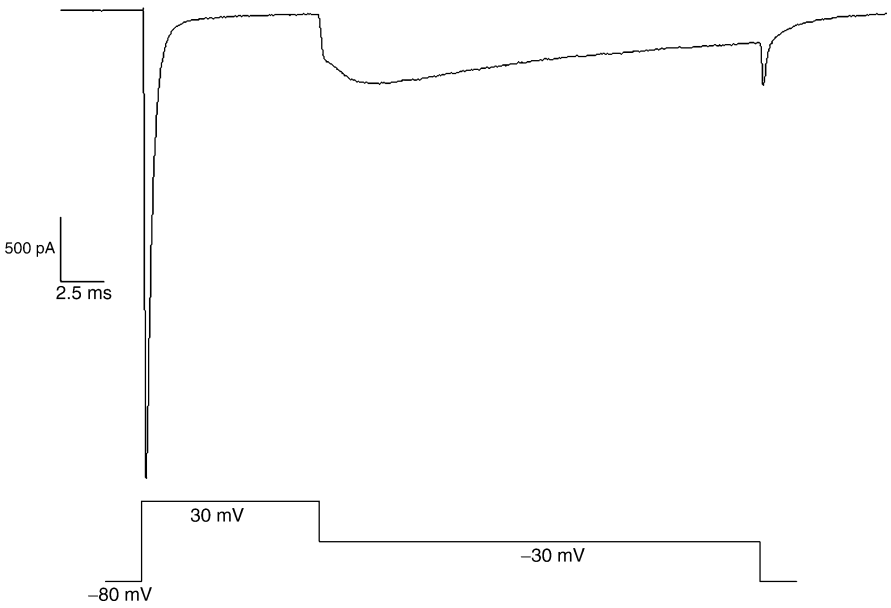

Fig. 2.8 *Resurgent Na^+ current.* Resurgent Na^+ current recorded using the whole-cell patch-clamp technique, holding a cell expressing VGSCs to a depolarized voltage (prepulse) to inactivate Na^+ current, followed by a test pulse to a less depolarized voltage. Resurgent Na^+ current is observed during the test pulse. Notice the similarity of this protocol to that described in Fig. 2.5, but with a difference in the timescale and the shape of the Na^+ currents recorded during the test pulse

VGSC β Subunits Are Cell Adhesion Molecules with Ion Channel–Dependent and Ion Channel–Independent Functions

As shown in Fig. 2.1, VGSCs, VGCCs, and VGPCs have accessory subunits that do not form the ion-conducting pore, yet are essential for normal channel behavior. The accessory subunits of VGSCs are unique compared to those of VGCCs and VGPCs, in that they function as cell adhesion molecules (CAMs) in addition to modulating the channel pore. Thus, these multifunctional members of the voltage-gated ion channel family are proposed to have specialized functions that may go beyond ion conduction.

VGSC β1–β4, encoded by *SCN1B–SCN4B*, are type I transmembrane proteins with similar structure: an extracellular amino-terminus containing a V-type immunoglobulin (Ig) fold, a single transmembrane domain, and a short intracellular carboxyl-terminus. Of the four VGSC β subunits, to date, only *SCN1B* and *SCN3B* have been found to be expressed as alternate mRNA splice variants. *SCN1B* can be expressed as two different polypeptides, β1 and β1B, generated through alternative mRNA splicing. In addition, both *SCN1B* and *SCN3B* can be

expressed as splice variants that differ in their 3′ untranslated regions, suggesting complex transcriptional regulation. β1B contains the identical Ig fold domain as β1, but lacks a transmembrane domain. Thus, this variant is a secreted protein. For the transmembrane variant, β1, both the Ig fold and the intracellular carboxyl-terminus are important sites for α-β subunit interaction. In contrast, the soluble β1B protein may associate with α subunits only via the Ig loop domain.

VGSC β subunits have both α-subunit-dependent and α-subunit-independent functions. β subunits modulate Na^+ current in vitro and in vivo in a cell-type-specific manner, through various mechanisms: (1) β subunits modify the gating, voltage dependence, and kinetic properties of pore-forming α subunits. (2) β subunits, particularly β2, modulate VGSC cell surface expression. β1 and β3 subunits may mask endoplasmic reticulum retention motifs in VGSC α subunits, thereby promoting channel transport to the plasma membrane. In contrast, the last step in VGSC biosynthesis has been shown to be concomitant insertion in the plasma membrane and covalent association with β2 via disulfide bonding. (3) β subunits are CAMs of the Ig superfamily that serve to physically link VGSC α subunits with other CAMs as well as molecules involved in molecular scaffolding and intracellular signal transduction. (4) β subunits are substrates for sequential cleavage by the enzymes β-site amyloid precursor protein-cleaving enzyme 1 (BACE1), ADAM10, and γ-secretase. Sequential cleavage is postulated to release the Ig loop domain into the extracellular space and the intracellular domain (ICD) into the cytoplasm. The released extracellular domain may function as a soluble ligand for cell adhesion. It has been shown in vitro that the released β2 ICD translocates to the nucleus of transfected cells and functions there as a transcriptional regulator of VGSC α subunit expression. This processing by BACE1 and γ-secretase has been confirmed in vivo for β2 and β4, but not for β1 or β3. Thus, intracellular processing of the β subunits that are normally disulfide-linked to α may be clinically relevant, although additional experiments are required to test this hypothesis.

Most of the research on VGSC β subunits has focused on their ability to change the electrophysiololgical properties of α subunits in heterologous expression systems in vitro. However, it is clear that this experimental approach does not reliably predict the effects of β subunits on Na^+ current in vivo. Interestingly, at least for β1, electrophysiological modulation may not be its most important function in vivo. For example, in spite of a large literature showing dramatic Na^+ current modulation by β1 in heterologous cells, isolated neurons from Scn1b null mice show subtle, cell-type-specific differences in Na^+ current compared to cells isolated from wild-type littermates. This is true in spite of a very severe neurological phenotype that models Dravet syndrome, a severe pediatric epileptic encephalopathy. Thus, nonconducting functions of β subunits are proposed to play important roles in vivo.

The presence of a single V set Ig fold in the extracellular domain of each β subunit places them in the Ig family of CAMs, capable of extracellular homotypic and heterotypic interactions with other CAMs and extracellular matrix molecules (Table 2.2). These interactions can occur in *trans*, between molecules on adjacent cells, or in *cis*, between molecules on the same cell membrane. While the β subunit

Ig fold is the structural motif that mediates interaction between CAMs, the downstream effects of this association require the β subunit intracellular domain. Homotypic interactions in *trans* have been described for β1 and β2, resulting in recruitment of the cytoskeletal protein ankyrin to points of cell-cell contact. In β1, the site of interaction with ankyrin is the residue tyrosine 181. Despite a high homology between the amino acid sequences of β1 and β3, no homotypic cell adhesive properties have been shown for the latter. To date, β3 has been shown to associate heterotypically with neurofascin-186, but not with other β subunits or homotypically with itself. The cell adhesive properties of β4 have not been investigated.

What are the functional consequences of β subunits acting as CAMs? (1) β subunits, by interacting with other CAMs on adjacent cells in *trans*, produce cell-cell adhesion. This may occur at specialized domains of intercellular association where VGSCs play crucial functional roles such as paranodal junctions of nodes of Ranvier in myelinated axons or cardiac intercalated disks. β1-β1 *trans* cell adhesive interactions have also been proposed to play important roles in axonal fasciculation. (2) Through *cis* interactions, β subunits may serve to link α subunits with other CAMs in particular subcellular domains. This association is postulated to increase the half-life of VGSC α subunits at the plasma membrane by tethering and thus reduction of intracellular channel recycling. Evidence for this is provided by the observation that cell surface expression of TTX-sensitive VGSCs, including expressing at nodes of Ranvier, is reduced in *Scn2b* null mice. In addition, the VGSC Nav1.6 is normally expressed at the axon initial segment of wild-type mouse cerebellar granule neurons. However, in Scn1b null mice, the predominant VGSC α subunit in this region is Nav1.1, suggesting that the absence of β1-mediated cell adhesive interactions alters the VGSC α subunit present at this important functional domain. In addition, β subunit-mediated cell adhesive interactions may modify Na^+ current via association of VGSCs with other CAMs, cytoskeletal, and signaling molecules. (3) β subunits modulate cellular migration and neurite extension. Both in vitro and ex vivo experiments have shown that both β1 and β4 promote neurite outgrowth, while β2 inhibits it. Thus, β subunit-mediated regulation of neurite outgrowth may be important in developmental processes like neuronal migration and axon pathfinding. It is known that the binding partner of β1 for this signaling can be another β1 molecule on an adjacent neuron or glial cell in *trans* or soluble β1B that has been secreted from an adjacent cell. In addition, requirements for β1-mediated promotion of neurite outgrowth in cerebellar granule neurons include TTX-sensitive Na^+ current mediated by Nav1.6, the CAM contactin, and the tyrosine kinase fyn. β1B is a secreted protein expressed predominantly during fetal brain development. This splice variant is proposed to form concentration gradients that serve as axon guidance cues during the development of neuronal circuits. The critical role of β1/β1B in CNS development is highlighted by the findings of defasciculation of the corticospinal tract, defasciculation of cerebellar parallel fibers, and abnormal migration of cerebellar granule and hippocampal neurons, as well as the severe and ultimately fatal neurological phenotype of *Scn1b* null mice.

VGSCs Are Modulated by Posttranslational Modification and Interaction with Other Proteins

1. Posttranslational Modification: Both VGSC α and β subunits are subject to multiple posttranslational modifications. VGSC α subunits can be phosphorylated by protein kinase A, protein kinase C, Ca^{2+}-calmodulin-dependent kinase II (CaMKII), p38 MAPK, and ERK1/2 mitogen-activated protein kinase at multiple serine residues in the intracellular loop regions. Fyn kinase, and possibly other members of the Src-family kinases, phosphorylates tyrosine residues on specific VGSC α subunits. Phosphatases, including calcineurin, PP2A, receptor phosphoprotein tyrosine phosphatase-β, and PTPH1 counter the action of kinases on VGSCs. Protein phosphorylation results in subunit-specific and cell-type-specific changes in current characteristics, including current amplitude, voltage dependence of current activation and/or inactivation, and rate of recovery from inactivation. In addition, phosphorylation can affect the level of channel protein expressed at the cell membrane. In addition to being phosphoproteins, VGSC α subunits are glycoproteins. N-linked glycosylation of these subunits takes place at the S5–S6 extracellular loop of DI. The presence of sialic acid in this region is required for appropriate electrophysiological modulation.

VGSC β1 subunits contain an intracellular tyrosine residue (Y181), whose phosphorylation controls the ability of β1 to associate with the cytoskeletal protein ankyrin as well as modulates the subcellular localization of β1 subunits in cardiomyocytes. β3 contains a tyrosine residue in the equivalent position, but its phosphorylation and ability to associate with ankyrin have not been demonstrated. The interaction of β1 in a protein complex with tyrosine kinases and RPTPβ in some tissues may provide a "yin-yang" mechanism of signal transduction-mediated protein phosphorylation and dephosphorylation. A cysteine residue at position 162 in β1 is a putative palmitoylation site, but the importance of this possible modification is unknown. Similar to VGSC α subunits, β subunits are also glycoproteins, with carbohydrates comprising approximately 33% of their molecular mass. Multiple sites of N-linked glycosylation for all five β subunits are located in the extracellular Ig domain, and glycosylation is required for normal electrophysiological modulation of α subunits.

2. VGSCs Reside in Large Protein Complexes. VGSC α and β subunits associate in complex with multiple proteins (Table 2.2) including molecules that function in signal transduction, cell adhesion, and cytoskeletal modulation. The identities of specific proteins composing a given VGSC complex are cell-type-specific and subcellular-domain-specific. Some interactions are specific to a particular VGSC subunit isoform. In vivo experiments have shown that the interaction of VGSC α subunits with $ankyrin_G$ is critical to the control of their subcellular localization, both in the heart and the CNS. In the CNS, interactions with Nr-CAM and neurofascin also contribute to channel subcellular localization. The interactions of both α and β subunits with extracellular matrix and cytoskeletal proteins are thought to help stabilize them at the plasma membrane, perhaps by inhibiting endocytosis and thus prolonging their half-life at the cell surface. The association

of α subunits with calmodulin and CaMKII also helps to stabilize their presence at the plasma membrane. $Na_v1.4$ and $Na_v1.5$ contain a PDZ domain binding motif at their carboxyl-termini that allow them to interact with proteins that have a PDZ motif, including Pdzd2 and members of the syntrophin family. VGSC α subunits are removed from the cell surface by two non-mutually exclusive mechanisms: endocytosis through association with caveolin-3 and synaptotagmin, and degradation by ubiquitination and the proteosome system, mediated in part by interaction with the Nedd-4-like ubiquitin-protein ligases.

The majority of studies published on protein-protein interactions of VGSC β subunits have focused on β1. Since β1B shares the Ig loop domain of β1, it is likely that it shares many of the same interactions with CAMs and extracellular matrix proteins as β1 in vivo. In vitro experiments show that tenascin-R repels fibroblasts expressing β1 or β2 in the absence of pore-forming α subunits. Both β1 and β2 associate with $ankyrin_B$ and $ankyrin_G$ in response to extracellular cell-cell adhesion. β1 binding partners include contactin, neurofascin-186, neurofascin-155, NrCAM, VGSC β2, and N-cadherin. The interaction of β1 with contactin and with VGSC β2 enhances its ability to increase the cell surface expression of α subunits. Interestingly, β1 subunits also associate with proteins normally associated with other voltage-gated ion channels. For example, in cardiac myocytes, β1 interacts with the VGPC subunits $K_v4.2$, $K_v4.3$, and KChIP2, suggesting that β subunits may act to coordinate Na^+ and K^+ currents in heart.

Abnormalities in VGSC Function Can Result in Human Disease

Mutations in genes encoding VGSC α and β subunits are associated with human disease, including skeletal muscle paralysis, epilepsy, cardiac arrhythmia, and neuropathic pain (Table 2.3). The first of the channelopathies to be discovered were the periodic paralyses of skeletal muscle in 1990, resulting from mutations in the inactivation gate, the inactivation gate receptor region, and the voltage sensors of *SCN4A* skeletal muscle VGSC a subunits. In most cases of channelopathies, only a single mutant allele, resulting in haploinsufficiency, is required to produce pathophysiology. The most dramatic example of this is haploinsufficiency of *SCN1A* resulting in Dravet syndrome, a severe pediatric epileptic encephalopathy. The genetic abnormalities most frequently found in VGSC α subunit genes are missense and nonsense mutations, but they can also include deletions, frameshift mutations, splice site mutations, mutations in the untranslated regions, and gene deletions. Mutations of VGSC α subunit genes can result in either gain or loss of function, as exemplified by mutations in *SCN5A* that result in long QT syndrome (gain of function) or Brugada syndrome (loss of function), two types of cardiac arrhythmia. Interestingly, there are reported cases where the same VGSC mutation results in either of these two diseases within the same pedigree. Mutations in *SCN9A*, encoding $Na_v1.7$, are associated with both gain and loss of neuropathic pain. *SCN9A* loss of function also results in anosmia, or failure of the sense of smell. It is postulated that changes in Na^+ current caused by a given mutation can have

Table 2.3 Human diseases associated with VGSC mutations

VGSC subunit	Diseases
SCN1A, $Na_v1.1$	Genetic epilepsy with febrile seizures plus (GEFS+), including Dravet syndrome
	Familial hemiplegic migraine
	Familial autism
SCN2A, $Na_v1.2$	Benign familial neonatal-infantile convulsions
	GEFS+, including Dravet syndrome
	Familial autism
SCN3A, $Na_v1.3$	Partial epilepsy
SCN4A, $Na_v1.4$	Potassium-aggravated myotonia
	Paramyotonia congenita
	Myotonia permanens
	Atypical myotonia congenita
	Hyperkalemic periodic paralysis
	Hypokalemic periodic paralysis
	Normokalemic periodic paralysis
	Congenital myasthenic syndrome
SCN5A, $Na_v1.5$	Long QT syndrome
	Brugada syndrome
	Progressive cardiac conduction disease
	Nonprogressive cardiac conduction block
	Paroxysmal familial ventricular fibrillation
	Sick sinus syndrome
	Dilated cardiomyopathy
	Atrial fibrillation
	Sudden infant death syndrome
SCN8A, $Na_v1.6$	Cerebellar atrophy, ataxia, and mental retardation
	Hereditary mental retardation
SCN9A, $Na_v1.7$	Inherited erythermalgia
	Paroxysmal extreme pain disorder
	Channelopathy-associated insensitivity to pain
	Chronic non-paroxysmal neuropathic pain
	GEFS+
	Familial febrile convulsions
	Anosmia
SCN10A, $Na_v1.8$	–
SCN11A, $Na_v1.9$	–
SCN1B, β1	Cardiac conduction disease
	Atrial fibrillation
	GEFS+, including Dravet syndrome temporal lobe epilepsy
SCN1B, β1B	Cardiac conduction disease
	Brugada syndrome
SCN2B, β2	Atrial fibrillation

(*continued*)

Table 2.3 (continued)

VGSC subunit	Diseases
SCN3B, β3	Idiopathic ventricular fibrillation
	Sudden infant death syndrome
	Brugada syndrome
	Atrial fibrillation
	Cardiac conduction disease
SCN4B, β4	Long QT syndrome
	Sudden infant death syndrome

different excitability phenotypes depending on subtle differences in interactions between ion channel subunits and their associated proteins, as commented above. For this reason, the genetic background of the patient is critical to disease phenotype. To date, no human pathologies have been associated with mutations in the genes for *SCN10A*, encoding $Na_v1.8$ or *SCN11A*, encoding $Na_v1.9$. In spite of this, *Scn10a* and *Scn11a* null mice exhibit moderate sensory perception deficits, suggesting that links to human diseases may be identified in the future.

All the diseases associated to date with mutations in genes encoding VGSC β subunits are episodic, or paroxysmal, in nature, and the reported mutations are missense, nonsense, or generate small deletions, resulting in gain or loss of function. The majority of reported cases are heterozygous probands with incomplete penetrance. Consistent with its wide tissue distribution, heterozygous mutations in *SCN1B* result in both the spectrum of epilepsies represented by genetic (generalized) epilepsy with febrile seizure plus (GEFS+) and cardiac arrhythmia. Interestingly, the same *SCN1B* mutation has been shown to be associated with either phenotype (temporal lobe epilepsy and atrial fibrillation) in different families. One patient with a homozygous loss-of-function mutation in *SCN1B* presented with Dravet syndrome, the most severe pediatric encephalopathy on the $GEFS^+$ spectrum, a phenotype similar to that of the *Scn1b* null mice. These mice also exhibit cardiac abnormalities. For reasons that are not yet understood, $Scn1b^{+/-}$ mice appear to be completely healthy with normal life spans, although this difference from human patients may be explained by genetic background differences. All reported patients to date with mutations in other β subunit encoding genes have presented with cardiac pathologies. Consistent with this, *Scn3b* null mice and a *Scn4b* hypomorphic mouse strain exhibit cardiac abnormalities, but not epilepsy. The cardiac phenotype of the *Scn2b* null mice has not been characterized. However, their phenotype appears to be completely healthy. One interesting aspect of this mouse model is that it is neuroprotective both in the CNS (in a model of multiple sclerosis) and the PNS (in models of chronic pain). The mechanism for this neuroprotection is postulated that β2 acts as a chaperone for TTX-sensitive VGSC α subunits, particularly of $Na_v1.6$, to the neuronal cell surface. This function is proposed to be critical following demyelination or other axonal damage when VGSC expression is upregulated. Because $Na_v1.6$ generates persistent Na^+ current, the increase of this channel protein at the cell surface is thought to result in the

accumulation of Na^+ inside the axon, driving the Na/Ca exchanger to reverse its function and raise intracellular Ca^{2+} levels. This results in the activation of cascades that cause axonal degeneration. For this reason, the potential neuroprotective function of *SCN2B* reduction in humans as well as the possibility of human mutations contributing to neurodegenerative disease need to be investigated.

The clinical importance of the multiple interactions between VGSC subunits and their associated proteins for proper functioning of the channel complex is supported by the observation that mutations in a number of these associated proteins result in phenotypes that are highly similar to those due to direct mutations in VGSC subunits. The best-known examples of this are Brugada syndrome cases due to mutations in the genes encoding GPD1L and $K_v4.3$, and long QT syndrome or long QT syndrome-like patients with mutations in the genes encoding caveolin 3, α1-syntrophin, and $ankyrin_G$.

A growing body of evidence suggests that VGSCs may play a role in cancer pathogenesis, especially in metastasis. Multiple cancer cell types, including breast cancer, prostate cancer, lymphoma, lung cancer, mesothelioma, neuroblastoma, and melanoma cells, express voltage-gated ion channels, including VGSCs. In vitro experiments have shown that breast cancer cells with a high metastatic potential express high levels of the neonatal splice variant of $Na_v1.5$ and low levels of β1. Their weakly metastatic counterparts express low levels of $Na_v1.5$ and high levels of β1. The increased expression of neonatal $Na_v1.5$ in metastatic breast cancer cells has been confirmed ex vivo. Similarly, highly metastatic prostate cancer cells show elevated expression of the neonatal splice variant of $Na_v1.7$ in vitro, and ex vivo experiments have confirmed that this upregulation correlates with metastatic potential. Similar to the mechanisms proposed for VGSCs in neurodegeneration, VGSCs in cancer cells are proposed to generate persistent Na^+ current that leads to downstream Ca^{2+}-dependent cascades. Importantly, all of these data must be confirmed in vivo. A high level expression of β1 in cancer cells does not necessarily predict a low metastatic potential, since strongly metastatic prostate cancer cell lines express higher levels of *SCN1B* mRNA than more weakly metastatic cells. Interestingly, the transcriptional regulators of VGSC subunit expression, REST and p53, are a candidate oncogene and a cancer suppressor gene, respectively, lending further support to the idea of VGSC involvement in cancer metastasis.

VGSCs Can Be Modulated by Naturally Occurring Toxins and by Therapeutic Agents

VGSC α subunits can be divided in two groups, depending on their affinity for the toxin tetrodotoxin (TTX), derived from puffer fish (fugu), which irreversibly blocks the α subunit ion-conducting pore. Channels that are blocked by nanomolar concentrations of TTX are called "TTX-sensitive" channels and include $Na_v1.1$, $Na_v1.2$, $Na_v1.3$, $Na_v1.4$, $Na_v1.6$, and $Na_v1.7$. The remaining α subunits ($Na_v1.5$, $Na_v1.8$, and $Na_v1.9$) can still be blocked by TTX, but require micromolar concentrations to do so, and are thus designated "TTX-resistant." The receptor site for

Table 2.4 Toxins interacting with VGSCs

Receptor site	Toxins	Domains	Functional effect
Site 1	Tetrodotoxin	IS5–S6, IIS5–S6, IIIS5–S6, IVS5-S6,	Pore block
	Saxitoxin		
	μ-Conotoxin		
Site 2	Batrachotoxin	IS6, IVS6	Enhanced activation and inactivation block
	Veratridine		
	Grayanotoxin		
	Aconitine		
Site 3	α-Scorpion toxins	IS5–S6, IVS3–S4, IVS5–S6	Slowed inactivation
	Sea anemone toxins		
	Atrachotoxins		
Site 4	β-Scorpion toxins	IIS1–S2, IIS3–S4	Enhanced activation and reduced peak current
	Huwentoxin-IV		Enhanced closed state
Site 5	Brevetoxins	IS6, IVS5	Enhanced activation and inactivation block
	Ciguatoxins		
Site 6	δ-Conotoxin	IVS3–S4	Slowed inactivation
–	μO-Conotoxin	IIS3–S4, IIIS5–S6	Reduced sodium conductance
–	ProTX-II	IIS3	Enhanced closed state

TTX (called receptor site 1) is composed of amino acids in the pore-loop region that form the ion selectivity filter. At this same site, two other types of pore-blocking toxins can bind: saxitoxin, produced by marine dinoflagellates and sometimes consumed by humans by eating clams or mussels, and μ-conotoxins, derived from cone snails. Clinically, poisoning with these toxins results in paralysis, autonomic symptoms, and sensory abnormalities. In addition to receptor site 1, there are five other regions of the VGSC α subunit (sites 2–6) where toxins can bind. Most of these are clustered in the region of each homologous domain between segments S4 and S6. All toxins in this group are gating modifier toxins that enhance VGSC activity through mechanisms that include persistent or enhanced channel activation, slowed channel inactivation, and voltage-sensor trapping. These toxins include grayanotoxins, veratridine, acotinine, batrachotoxin (all of which bind to α subunits in the open state and trap them in the open state even after repolarization), brevetoxins, ciguatoxins, α- and β-scorpion toxins, sea anemone toxins, some spider toxins, and δ-conotoxins (Table 2.4).

VGSCs are also the target for multiple therapeutic agents, including local anesthetic, antiarrhythmic, and anticonvulsant drugs, all of which effectively reduce Na^+ current. Given the central role of VGSCs in the generation of action potentials, many of these drugs are also useful in the management of pain and bipolar disorder. The antiepileptic drugs phenytoin and carbamazepine primarily

target VGSCs as their mechanism of action, blocking them in a voltage-dependent and frequency-dependent manner. For some other antiepileptic drugs, blocking VGSC α subunits is only one of many mechanisms of action. Such drugs include valproate, lamotrigine, zonisamide, topiramate, lacosamide, and ethosuximide. It is important to note that many patients with $GEFS^+$ spectrum disorders secondary to genetic abnormalities of *SCN1A* are resistant to treatment with phenytoin and carbamazepine. Unfortunately, for many of these patients, VGSC drugs actually worsen seizure severity. Evidence from some mouse models suggests that $Na_v1.1$ is the predominant VGSC α subunit expressed in subtypes of inhibitory neurons in the hippocampus. When $GEFS^+$ patients are treated with antiepileptic drugs whose primary mechanism of action is VGSC blockade, these inhibitory neurons may lose their small amount of remaining Na^+ current, resulting in reduced inhibitory firing and hyperexcitability of the neuronal network, although this has yet to be proven in human neurons. Human patients with these disorders respond better to antiepileptic drugs that have other mechanisms of action. Interestingly, for reasons that are poorly understood, phenytoin has been shown to act as a chaperone for mutated $Na_v1.1$ proteins that are trafficking deficient as a result of protein misfolding, possibly opening the door to therapeutic solutions for trafficking deficient VGSC disease mutations.

Cardiac drugs that block VGSCs are classified as class I antiarrhythmics. Of these agents flecainide, lidocaine, mexiletine, propafenone, and tocainide act almost exclusively on VGSCs. Disopyramide, procainamide, and quinidine block VGPCs in addition to their effect on VGSCs. Like phenytoin and carbamazepine, these agents block VGSC α subunits in a use-dependence manner. Similar to cases of $GEFS^+$ secondary to *SCN1A* mutations, the use of antiarrhythmic agents that block Na^+ current can worsen the clinical condition in patients with arrhythmia secondary to loss-of-function VGSC mutations.

To date, there are no known toxins or medications that target VGSC β subunits. However, the presence of β subunits modulates the response of VGSC α subunits to phenytoin, carbamazepine, flecainide, and lidocaine. This information is an important consideration for physicians making decisions about drug treatment for patients with inherited epilepsy or cardiac arrhythmia resulting from VGSC β subunit gene mutations.

Outlook

Despite the wealth of information we have learned about VGSCs over the past decades, many exciting questions remain. Multiple studies have characterized the tissue expression of VGSC subunits in different animal species, but few studies have been carried out in human samples. By the same token, many of the reported expression/localization studies used reverse transcriptase PCR and need to be validated with immunohistochemistry and biochemistry. The genetic mechanisms controlling the expression of the different VGSC subunits and their splice variants are waiting to be unraveled. There is still uncertainty regarding the structural

changes that VGSC subunits undergo at each state of the channel, especially because, unlike K^+ channels, VGSC subunits have been very difficult to process for X-ray crystallography. The implications of many of the posttranslational modifications and protein interactions of VGSC subunits are still not clear, and more studies on this area are necessary.

The discovery of the ability of β subunits to act as CAMs, resulting in α-subunit-independent functions, has opened an entire new avenue of research in the field of VGSC biology. The developmental roles of β1 and β2 are beginning to be delineated, but those of the other β subunits still await characterization. Mutations in some CAMs of the Ig superfamily have been associated with psychiatric diseases. Given the high comorbidity of epilepsy and psychiatric disorders, the possibility must be explored that VGSC dysfunction (including mutations in β subunit function) contributes to these disease phenotypes. Additional evidence to support this hypothesis includes the association of mutations in genes for VGSC α subunits with autism and the use of Na^+ channel blockers in the treatment of bipolar disorder. Even though we have learned a lot about the genetics of epilepsies due to mutations of genes encoding VGSC subunits, such information is of limited clinical value at the present time. Prospective studies need to be designed to test the utility of genetic studies in predicting the need for future anticonvulsive treatment and, if so, the choice of medication, at the time of first seizure. Human and animal studies will also need to determine modifying factors for the phenotype of *SCN1B* mutations to explain why the resulting diseases have incomplete penetrance and why some pedigrees show cardiac compromise while others suffer from epilepsy. The idea of VGSC β2 downregulation being neuroprotective awaits confirmation in human diseases. By the same token, the possibility of using VGSC blocking drugs to reduce the frequency of metastasis must be tested in the clinical setting. The potential benefit of drugs that target VGSC β subunits is an unexplored subject so far, but one that holds the promise of widely increasing our therapeutic arsenal to address a variety of human diseases, including epilepsy, cardiac arrhythmia, chronic pain, and even cancer.

Important studies to investigate the role of voltage-gated ion channels in human disease are now being performed using a novel and remarkable technique that overcomes many of the limitations inherent in using heterologous systems and/or animal models to investigate channel physiology. We refer here to the induced pluripotent stem cell (IPSC) technique. In this method, a skin biopsy is obtained from a patient with an inherited ion channelopathy like epilepsy or cardiac arrhythmia. Skin fibroblasts are isolated from the biopsy and virally transduced with a defined cocktail of transcription factors to induce pluripotency – or the ability of the cell to become any tissue in the human body. We call these cells induced pluripotent stem cells, or iPSCs. iPSCs can be differentiated into any cell type, including neurons and cardiomyocytes. These cells can then be used for experiments that include biochemistry, molecular biology, electrophysiology, fluorescent imaging, and pharmacology or drug screening. This extremely powerful technique is currently being used to study the mechanisms by which mutations in ion channels result in human disease. In addition, and most importantly, iPSCs are being used to

develop novel and personalized medical treatments. For example, we know that seizure severity in patients with Dravet syndrome is often worsened with traditional antiepileptic drugs that target VGSCs. Using the iPSC technique, novel therapeutic agents can be tested on the patient's neurons in the culture dish without administering the drug to the patient and risking harmful side effects.

In summary, the field of voltage-gated ion channels is exciting, both literally and figuratively. Voltage-gated ion channels control the electrical excitability of brain, spinal cord, heart, skeletal muscle, and peripheral nerve. In addition, voltage-gated ion channel accessory subunits may have functions that are independent of ion conduction. The Human Genome Project has revealed that mutations in voltage-gated ion channels result in devastating diseases, including epilepsy, cardiac arrhythmia, paralysis, and neuropathic pain. Important drugs in common use for these diseases target voltage-gated ion channels. New avenues of research, including use of the iPSC technique, are predicted to lead to novel and personalized therapeutic agents in the future.

Further Reading

Beneski D, Catterall WA (1980) Covalent labeling of protein components of the sodium channel with a photoactivable derivative of scorpion toxin. Proc Natl Acad Sci USA 77:639–642

Brackenbury WJ, Djamgoz MBA, Isom LL (2008) An emerging role for voltage-gated Na^+ channels in cellular migration: regulation of central nervous system development and potentiation of invasive cancers. Neuroscientist 14:571–583

Catterall WA (1980) Neurotoxins that act on voltage-sensitive sodium channels. Annu Rev Pharmacol Toxicol 20:l5–l43

Catterall WA (1984) The molecular basis of neuronal excitability. Science 223:653–661

Catterall WA (1986) Voltage-dependent gating of sodium channels: correlating structure and function. Trends Neurosci 9:7–10

Catterall WA, Goldin AL, Waxman SG (2005) International union of pharmacology. XLVII. Nomenclature and structure-function relationships of voltage-gated sodium channels. Pharmacol Rev 57:397–409

Catterall WA, Cestèle S, Yarov-Yarovoy V, Yu FH, Konoki K, Scheuer T (2007) Voltage-gated ion channels and gating modifier toxins. Toxicon 49:124–141

Curtis BM, Catterall WA (1984) Purification of the calcium antagonist receptor of the voltage-sensitive calcium channel from skeletal muscle transverse tubules. Biochemistry 23: 2113–2118

Goldin AL, Snutch T, Lubbert H, Dowsett A, Marshall J, Auld V, Downey W, Fritz LC, Lester HA, Dunn R, Catterall WA, Davidson N (1986) Messenger RNA coding for only the? subunit of the rat brain Na channel is sufficient for expression of functional channels in Xenopus oocytes. Proc Natl Acad Sci USA 83:7503–7507

Hartshorne RP, Catterall WA (1981) Purification of the saxitoxin receptor of the sodium channel from mammalian brain. Proc Natl Acad Sci USA 78:4620–4624

Hartshorne RP, Messner DJ, Coppersmith JC, Catterall WA (1982) The saxitoxin receptor of the sodium channel from rat brain. Evidence for two nonidentical β subunits. J Biol Chem 257:13888–13891

Hartshorne RP, Keller BU, Talvenheimo JA, Catterall WA, Montal M (1985) Functional reconstitution of the purified brain sodium channel in planar lipid bilayers. Proc Natl Acad Sci USA 82:240–244

Hille B (2001) Ion channels of excitable membranes, 3rd edn. Sinauer, Sunderland, MA

Hughes A (2010) Cardiac sodium channel Nav1.5 and interacting proteins: physiology and pathology. J Mol Cell Cardiol 48:2–11

Isom LL, De Jongh KS, Patton DE, Reber BFX, Offord J, Charbonneau H, Walsh K, Goldin AL, Catterall WA (1992) Primary structure and functional expression of the? 1 subunit of the rat brain sodium channel. Science 256:839–842

Isom LL, Ragsdale DS, De Jongh KS, Westenbroek RE, Reber BFX, Scheuer T, Catterall WA (1995) Structure and function of the? 2 subunit of brain sodium channels, a transmembrane glycoprotein with a CAM-motif. Cell 83:433–442

Li M, West JW, Numann R, Murphy BJ, Scheuer T, Catterall WA (1993) Convergent regulation of Na+ channels by protein kinase C and cAMP-dependent protein kinase. Science 261: 1439–1442

Mantegazza M, Curia G, Biagini G, Ragsdale DS, Avoli M (2010) Voltage-gated sodium channels as therapeutic targets in epilepsy and other neurological disorders. Lancet Neurol 9:413–424

Noda M, Ikeda T, Suzuki H, Takeshima H, Takahashi T, Kuno M, Numa S (1986a) Expression of functional sodium channels from cloned cDNA. Nature 322(6082):826–828

Noda M, Ikeda T, Suzuki H, Takeshima H, Takahashi T, Kuno M, Numa S (1986b) Existence of distinct sodium channel messenger RNAs in rat brain. Nature 320(6058):188–192, PubMed PMID: 3754035

Ogata N, Ohishi Y (2002) Molecular diversity of structure and function of the voltage-gated Na^+ channels. Jpn J Pharmacol 88:365–377

Patino GA, Isom LL (2010) Electrophysiology and beyond: multiple roles of Na^+ channel β subunits in development and disease. Neurosci Lett 486:53–55

Payandeh J, Scheuer T, Zheng N, Catterall WA (2011) The crystal structure of a voltage-gated sodium channel. Nature 475(7356):353–358

Ragsdale DS, McPhee JC, Scheuer T, Catterall WA (1994) Molecular determinants of state-dependent block of Na^+ channels by local anesthetics. Science 265:1724–1728

Scheuer T (2010) Regulation of sodium channel activity by phosphorylation. Semin Cell Dev Biol. doi:10.106/j.semcdb.2010.10.002

Talvenheimo JA, Tamkun MM, Catterall WA (1982) Reconstitution of neurotoxin-stimulated sodium transport by the voltage-sensitive sodium channel purified from rat brain. J Biol Chem 257:11868–11871

Vassilev PM, Scheuer T, Catterall WA (1988) Identification of an intracellular peptide segment involved in sodium channel inactivation. Science 241:1658–1661

Weiss J, Pyrski M, Jacobi E, Bufe B, Willnecker V, Schick B, Zizzari P, Gossage SJ, Greer CA, Leinders-Zufall T, Woods CG, Wood JN, Zufall F (2011) Loss-of-function mutations in sodium cannel Na(v)1.7 cause anosmia. Nature. doi:10.1038/nature09975

West JW, Patton DE, Scheuer T, Wang Y, Goldin AL, Catterall WA (1992) A cluster of hydrophobic amino acid residues required for fast Na^+ channel inactivation. Proc Natl Acad Sci USA 89:10910–10914

Yu FH, Mantegazza M, Westenbroek RE, Robbins CA, Kalume F, Burton KA, Spain WJ, McKnight GS, Scheuer T, Catterall WA (2006) Reduced sodium current in GABAergic interneurons in a mouse model of severe myoclonic epilepsy of infancy. Nature Neurosci 9(1142):1149